JOURNAL OF SOLID STATE CHEMISTRY 103, 30–37 (1993)

Phase Formation and Electronic Transport Properties in the Corundum (Ti_2O_3)–Ilmenite ($MgTiO_3$) System

A. B. SHEIKH AND J. T. S. IRVINE

Chemistry Department, Aberdeen University, Meston Walk, Aberdeen AB9 2UE, Scotland

Received April 21, 1992; in revised form July 30, 1992; accepted July 31, 1992

At high temperatures the Ti_2O_3–$MgTiO_3$ system shows extensive solid solution formation with an order/disorder transition between ilmenite- and corundum-type structures. At lower temperatures (<1000°C), there exists a large immiscibility dome, extending from $Mg_{0.9}Ti_{1.1}O_3$ to $Mg_{0.4}Ti_{1.6}O_3$. Although X-ray peak intensities indicate a gradual change from order to disorder with composition, there is a discontinuity at the ilmenite/corundum boundary. The relationship between unit cell parameters and composition generally obeys Vegard's Law, apart from a deviation close to the Ti_2O_3 end member. Above 180 K thermally activated conductivity is observed, with a discontinuity at the corundum/ilmenite boundary. At lower temperatures, a change in conductivity behavior occurs, with a linear relationship between log resistivity and temperature being found up to 30 K in samples with low Ti oxidation state.

Introduction

The electronic transport properties of the early first row transition metal oxides have been the subject of considerable interest. Several of the oxides of titanium exhibit metal–insulator transitions, including Ti_2O_3 (*1*, *2*), Ti_3O_5, and Ti_4O_7 (*3*). Superconducting transitions have been observed at 0.9 K in TiO (*4*) and at 13.6 K in the spinel $LiTi_2O_4$ (*5*), and an unusual insulator to metal transition was recently reported in the $(Mg, Ti)_3O_4$ spinel system (*6*).

Metal–insulator transitions in the sesquioxides of vanadium and titanium, both of which exhibit the corundum structure, have been extensively studied and considerable progress has been made in understanding the nature of these transitions (*7*). On cooling V_2O_3 doped with small amounts of Cr^{3+}, for example, two transitions may be observed; first from a nonmagnetic semiconductor to a metal at ~300 K and then from a metal to an antiferromagnetic insulator at ~160 K (*8*). In Ti_2O_3 a single metal–insulator transition is observed at about 500 K (*2*).

In the ternary MgO–TiO–O system there are a number of binary joins which may give rise to solid solution formation. These are associated with pseudobrookite (Ti_3O_5–$MgTi_2O_5$), spinel ($MgTi_2O_4$–Mg_2TiO_4), ilmenite (Ti_2O_3–$MgTiO_3$), and rocksalt (TiO–MgO) type structures (Fig. 1). Recent investigations have indicated solid solution formation in the spinel (*6*, *9*), ilmenite (*10*), and pseudobrookite systems (*11*).

In our recent experiments, which showed an anomalous resistivity transition in the spinel system, possibly indicative of superconductivity, ilmenite was frequently found as a minor impurity phase. In order to ascertain if the ilmenite was the phase responsible for the anomalous resistivity behavior, a careful study was made of the $MgTiO_3$–

0022-4596/93 $5.00

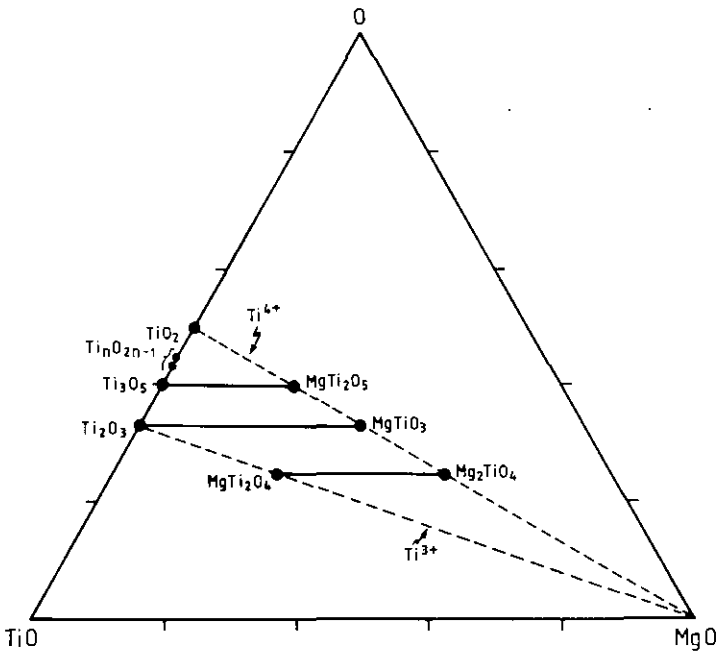

FIG. 1. Phase relationships in the system MgO–TiO–O.

Ti_2O_3 system. During the course of this investigation, a study of solid solution formation in this system was published (*10*); however, our findings indicate much more complex phase relationships than those reported in that study.

The Ti_2O_3, corundum, structure consists of an approximately hexagonally close-packed array of oxide ions with the metal ions occupying two-thirds of the octahedral interstices. The structure of ilmenite is related to that of corundum by the ordering of cations in two nonequivalent octahedral sites. In the $MgTiO_3$, ilmenite, end member, Mg and Ti are ordered into layers that alternate along the hexagonal c direction.

Experimental

Samples of composition $Mg_{1-y}Ti^{x+}_{1+y}O_3$ with an average Ti oxidation state $x = (4 + 2y)/(y + 1)$ were prepared using the following procedure. The raw materials MgO (BDH, AnalaR) and TiO_2 (Tioxide 99.95%) were dried at 700°C for 4 hr prior to being weighed, to ensure elimination of adsorbed H_2O and CO_2, particularly for MgO. Appropriate amounts of MgO, TiO_2, and Ti (Specpure, Johnson Matthey) were weighed out according to

$$(1 - y)\mathrm{MgO} + (2 + y)/2\ \mathrm{TiO_2} + y/2\ \mathrm{Ti} \rightarrow \mathrm{Mg_{1-y}Ti^{x+}_{1+y}O_3}.$$

These were mixed, ground together with acetone in an agate mortar, and when the acetone had evaporated, pressed into pellets. The pellets were placed in graphite boats and put into the center of an alumina tube furnace under a constant stream of argon. The temperature was slowly increased to 1400°C over 3 hr, and the samples reacted for 48 hr. The temperature was then reduced to room temperature over 4 hr before the pellets were removed from the furnace.

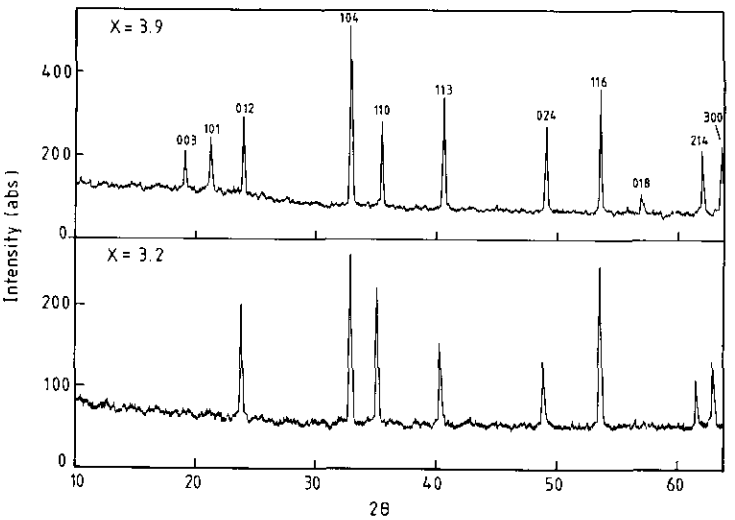

FIG. 2. X-ray powder diffraction patterns for samples with ilmenite (x = 3.9) and corundum (x = 3.2) structures.

Phase purity was determined by X-ray powder diffractometry using a Stoe Stadi linear psd system. Unit cell parameters were obtained by a least-squares fitting routine and peaks were integrated utilizing Stoe software.

Electrical measurements were performed using In/Ga electrodes, measuring parallel to the face of 1.2 cm diameter cylindrical pellets. Four-terminal dc resistance measurements down to 15 K were carried out on samples mounted on an Air Products helium cryotip with an Au (0.7% Fe)/Chromel thermocouple. The samples were cooled to about 15 K, held for about 30 min, then allowed to warm up to room temperature at a rate of 2 K min^{-1}. Galvanostatic control was achieved using a Farnell D100 power supply and reference electrode voltage difference was monitored using a Linseis 2021 recorder.

Two terminal ac impedance measurements using a Solartron 1250, 1286 impedance analysis system confirmed that the dc resistance pertained to the bulk of the ceramic, rather than to grain boundary or electrode effects (*12*). Impedance results were also used to convert four-terminal resistance values to resistivities via normalization of room temperature values.

Results

Samples with an average Ti oxidation state of 3.0–3.2 were single phase and gave rise to a corundum type structure. Those in the range 3.85–4.0 were also single phase but had the ilmenite type structure. Figure 2 shows a comparison of the ilmenite (x = 3.9) and corundum (x = 3.2) X-ray diffraction patterns. These are very similar, the main difference being that the ilmenite possesses two extra lines at low 2Θ values. Compositions with x = 3.3 − 3.8 were not single phase. X-ray diffraction showed small, but definite, peak splittings, indicating that these compositions contained a mixture of the ilmenite and the corundum phases. This important feature was not detected in earlier studies of this system (*10*).

In order to obtain single phases of compositions 3.3–3.8 it was necessary to quench

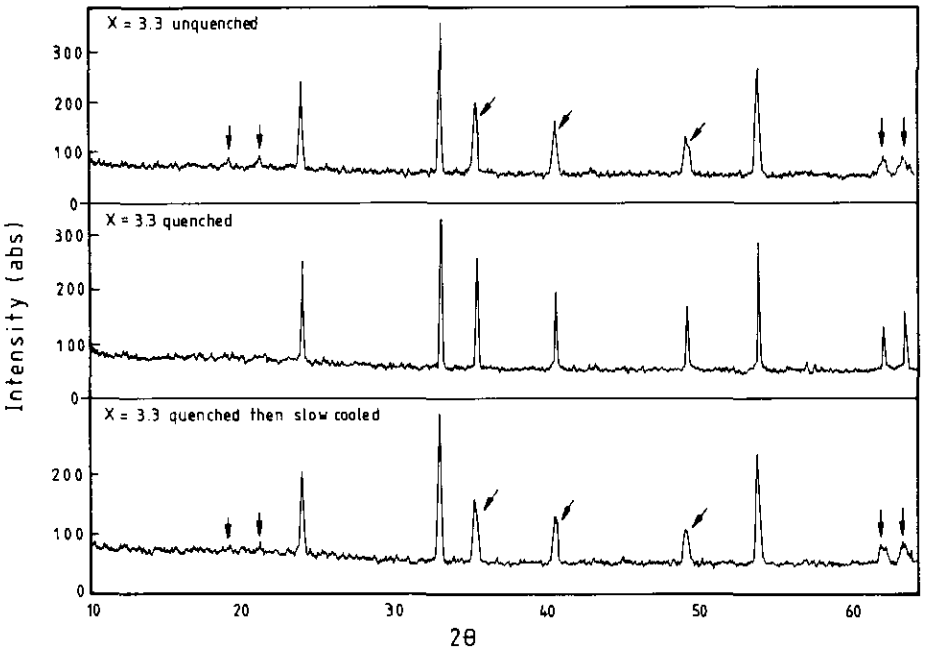

FIG. 3. Effect of quenching upon powder pattern of $x = 3.3$; arrows indicate additional lines due to ilmenite phase.

samples from high temperatures to room temperature under argon flow. Figure 3 shows how the powder pattern for a sample of $x = 3.3$ changes from showing the presence of two phases in the as-prepared sample to a single phase in a sample quenched from 800°C and back to two phases after low-temperature annealing.

A proposed phase diagram based on the results of these experiments is shown in Fig. 4. The most important feature of this phase diagram is the extensive immiscibility dome which ranges from $Mg_{0.9}Ti_{1.1}O_3$ to $Mg_{0.4}Ti_{1.6}O_3$ and up to 950°C. Such a feature is not unusual in an ilmenite–corundum system and has been reported in the system Fe_2O_3–$FeTiO_3$ (*13*). If the small difference between the ilmenite and corundum structures is ignored, then, at high temperatures, the solid solution can be regarded as continuous. Looking at the system more carefully, there is a clear transition, which could be detected, as a function both of composition and of temperature, Fig. 4. Although there was a gradual change in powder pattern as composition changed from $MgTiO_3$ toward Ti_2O_3, a discontinuous change in peak intensities occured at the boundary between ilmenite and corundum structures, Fig. 5; hence this boundary could be mapped out with confidence. This boundary appears to intercept the solvus close to $Mg_{0.5}Ti_{1.5}O_3$.

Unit cell lattice parameters generally show a linear dependence upon composition for single phase samples, in accord with Vegard's law (Fig. 6). A significant deviation from Vegard's law does occur, however, as x approaches 3 (Ti_2O_3). This deviation appears to be largely due to antiferromagnetic ordering in Ti_2O_3, as lattice parameters obtained at temperatures above the metal–insulator transition (*14*) deviate very much less from the behavior predicted by Vegard's law.

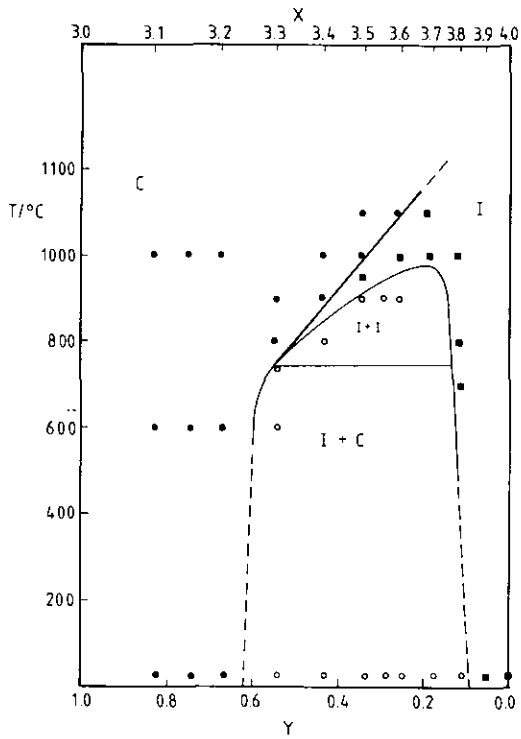

FIG. 4. Phase diagram for system Ti_2O_3–$MgTiO_3$: (I) ilmenite structure; (C) corundum structure.

The influence of small degrees of oxygen nonstoichiometry was investigated by preparing samples of varying oxygen stoichiometry for $x = 3.0$, 3.2, Table I. Detection of impurity phases by X-ray diffraction is not possible at levels up to the 2% level; however, changes in unit cell parameters can confirm solid solution formation. The small, essentially insignificant, changes in lattice parameter are in accord with the report by Andersson *et al.* (*15*), which stated that the oxygen content of Ti_2O_x was within the range $2.98 < x < 3.02$. It is clear that oxygen nonstoichiometry is not responsible for the deviation from Vegard's law discussed in the previous section.

Electrical measurements indicate fairly high electronic conductivity, in the range from 0.1 to 10 $ohm^{-1} \cdot cm^{-1}$ at 300 K. All samples show thermally activated hopping above 180 K. Activation energies increase with average oxidation state, showing a distinct step at the corundum/ilmenite transition, Fig. 7. At lower temperatures, a deviation from thermally activated hopping is observed across the system, with a distinct transition to a linear relationship between resistivity and temperature below about 30 K in some samples, Fig. 8.

Discussion

Due to the limited range of solid solution formation in furnance-cooled $Mg_{1-x}Ti_{1+x}O_3$, investigation of the relationship between composition and properties in such samples is of limited value. In this study we have utilized single-phase, quenched samples to allow investigation of composition–property relationships across the entire system.

The form of the immiscibility dome in Fig. 4 clearly indicates that a much wider range of compositions are stable to low temperature in the disordered, corundum phase than in the ordered, ilmenite phase. As composition moves toward $MgTiO_3$ the temperature

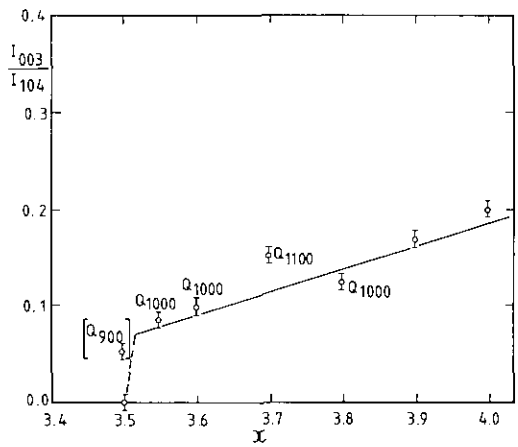

FIG. 5. Dependence of X-ray peak area for 003 reflection upon composition for single phase samples; Q_{1000} indicates sample quenched from 1000°C. Line corresponds to 1000°C isotherm.

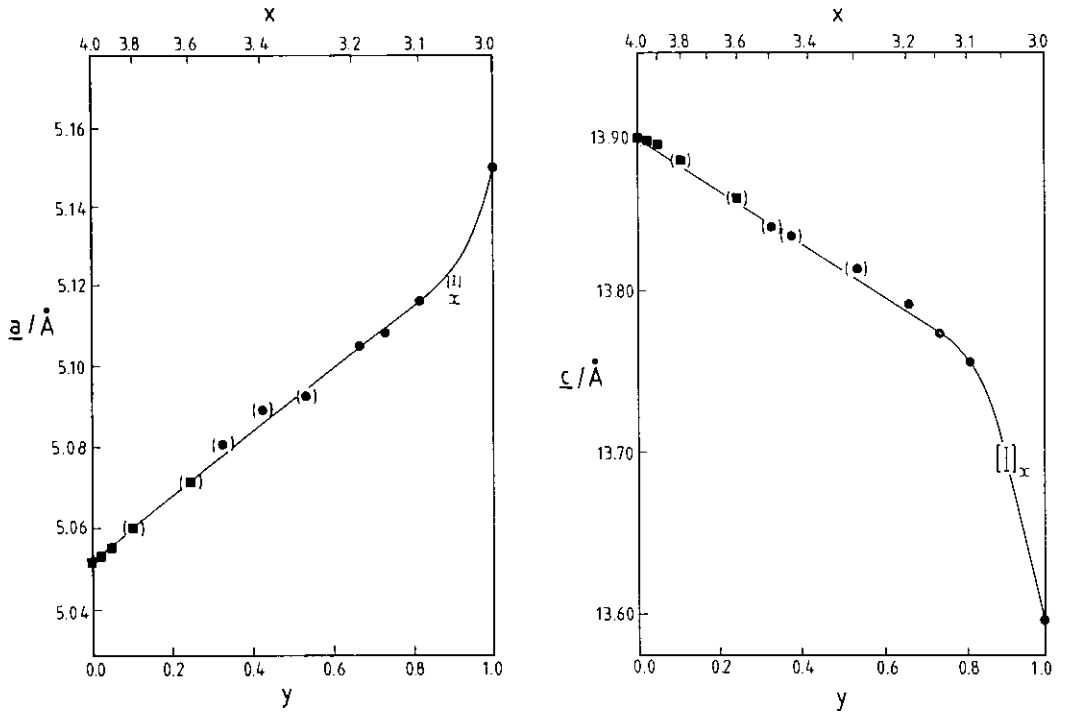

FIG. 6. Unit cell parameters as a function of composition, estimated standard deviations are within symbol size, parentheses indicate quenching: (●) corundum, (■) ilmenite, (×) from the literature (*10*).

of the order–disorder transition also increases; however, the transition does not extend to $MgTiO_3$. No evidence was found for such a transition by DTA, nor was there evidence for the disordered phase in quenched $MgTiO_3$. X-ray powder patterns indicate that there is a gradual increase in the extent of ordering in the ilmenite phase as the composition changes towards $MgTiO_3$, Fig. 5. There is, however, clear evidence that the transition from ilmenite to corundum is first order, both from X-ray peak intensities and from the discontinuity in conductivity activation energies when the boundary is crossed.

TABLE I

INFLUENCE OF OXYGEN NONSTOICHIOMETRY UPON UNIT CELL LATTICE PARAMETERS

x	O Content	a(Å)	c(Å)
3.0	3.02	5.155 (1)	13.623 (4)
3.0	3.00	5.154 (1)	13.613 (3)
3.0	2.98	5.159 (1)	13.600 (5)
3.2	3.01	5.103 (1)	13.778 (4)
3.2	3.00	5.106 (1)	13.791 (5)
3.2	2.99	5.110 (1)	13.767 (4)

Above 180 K linear Arrhenius plots were obtained for all compositions, consistent with a small polaron hopping mechanism. Activation energy increases with oxidation state of Ti in both the corundum and ilmenite regimes. The decrease in activation energy observed in crossing the boundary from corundum to ilmenite structures simply reflects the decrease in average jump distance due to ordering of Ti atoms. The deviation from linear Arrhenius behavior at low temperatures might be expected to be due to variable range

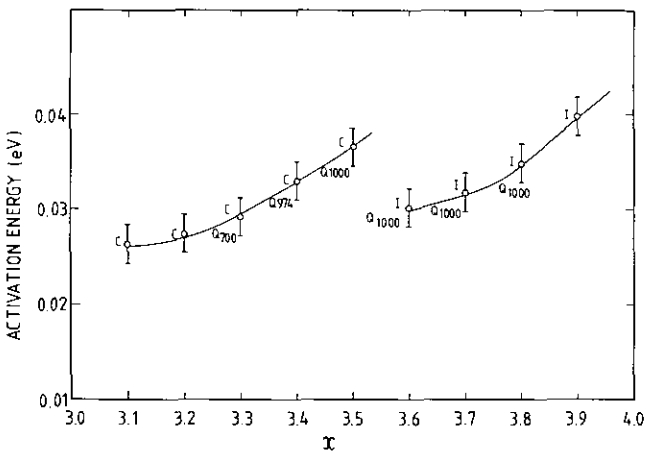

FIG. 7. Arrhenius activation energy as a function of composition, determined for $T > 180$ K.

hopping; however, the expected dependence upon $T^{-1/4}$ at low temperatures was not observed, with $\log \rho$ tending to a constant value at large $T^{-1/4}$, Fig. 8b. Instead, at low temperatures (<30 K) the logarithm of the resistivity appeared to increase linearly with temperature, Fig. 8a. Similar dependences have previously been observed for spinel titanates (*16*); however, a satisfactory model for this behavior has still to be proposed.

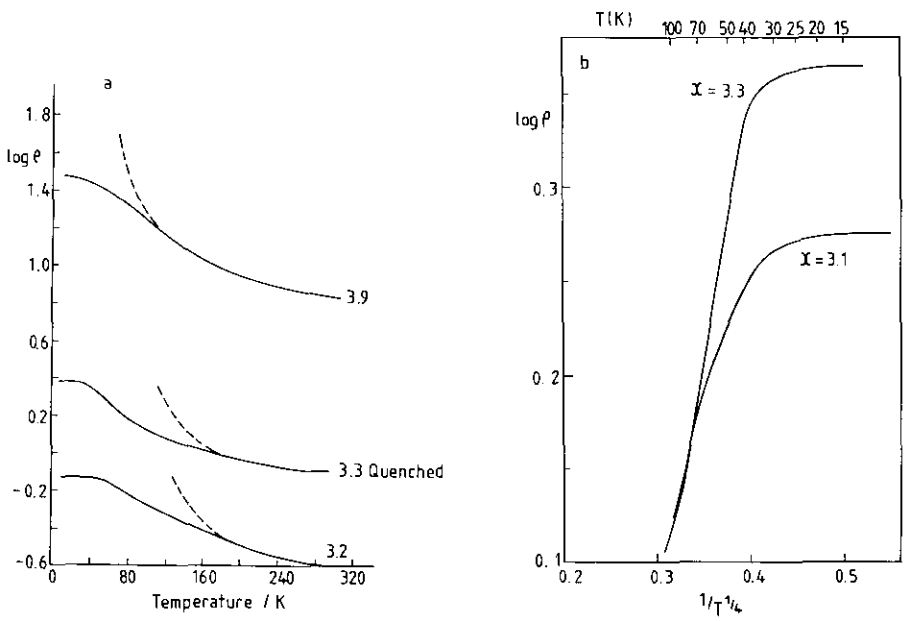

FIG. 8. Temperature dependence of resistivity: (a) log resistivity (ρ) plotted against T, where dashed lines indicate extrapolation of high temperature thermally activated hopping; (b) log resistivity plotted against $T^{-1/4}$.

Acknowledgments

We thank Tioxide plc and the SERC for a CASE research studentship (AS).

References

1. F. J. MORIN, *Bell System Tech. J.* **37,** 826 (1968).
2. L. L. VAN ZANDT, J. M. HONIG, AND J. B. GOODENOUGH, *J. Appl. Phys.* **39,** 594 (1968).
3. R. F. BARTHOLOMEW, AND D. R. FRANKEL, *Phys. Rev.* **187,** 828 (1969).
4. T. B. REED, M. D. BANUS, M. SJOSTRAND, AND P. H. KEESON, *J. Appl. Phys.* **43,** 2478 (1972).
5. D. C. JOHNSTON, *J. Low Temp. Phys.* **25,** 145 (1976).
6. T. J. COGLE, C. A. S. MATEUS, J. H. BINKS, AND J. T. S. IRVINE, *J. Mater. Chem.* **1,** 289 (1991).
7. M. YETHIRAJ, *J. Solid State Chem.* **88,** 53 (1990); T. F. ROSENBAUM AND S. A. CARTER, *J. Solid State Chem.* **88,** 94 (1990); J. SPALEK, *J. Solid State Chem.* **88,** 70 (1990); N. F. MOTT, *Philos. Mag.* **20,** 1 (1969).
8. F. J. HIMPSEL AND TH. FAUSTER, *Phys. Rev. Lett.* **49,** 1583 (1982).
9. A. FELTZ AND M. STEINBRUCK, *J. Less-Common Met.* **167,** 233 (1991).
10. A. FELTZ, M. STEINBRUCK, AND F. W. BREITBARTH, *Z. Anorg. Allg. Chem.* 137 **590,** (1990).
11. M. STEINBRUCK AND A. FELTZ, *Z. Anorg. Allg. Chem.* **594,** 157 (1991).
12. D. C. SINCLAIR, J. T. S. IRVINE, AND A. R. WEST, *Adv. Mater.* **2,** 132 (1990).
13. C. M. CARMICHAEL, *Proc. R. Soc. London Ser. A* **263,** 508 (1961); A. F. BUDDINGTON AND D. H. LINDSLEY, *J. Petrol.* **5,** 310 (1964).
14. R. E. NEWNHAM AND Y. M. DE HAAN, *Z. Kristallogr.* **117,** 235 (1962).
15. S. ANDERSSON, B. COLLEN, U. KUYLENSTIERNA, AND A. MAGNELI, *Acta Chem. Scand.* **11,** 1641 (1957).
16. A. B. SHEIKH, S. M. FRAY, A. A. FINCH, C. NAMGUNG, AND J. T. S. IRVINE, in preparation.